Alkaline electrolysis for green hydrogen production: techno-economic analysis of temperature influence and control

Lingkang Jin[a], Rafael Nogueira Nakashima[b], Gabriele Comodi[c] and Henrik Lund Frandsen[d]

[a] Department of Industrial Engineering and Mathematical Sciences (DIISM), Università Politecnica delle Marche, Ancona, Italy, l.jin@pm.univpm.it, CA
[b] Department of Energy Conversion and Storage, Technical University of Denmark (DTU), Building 310, Fysikvej, DK-2800 Lyngby, Denmark, rafnn@dtu.dk ,
[c] Department of Industrial Engineering and Mathematical Sciences (DIISM), Università Politecnica delle Marche, Ancona, Italy, g.comodi@staff.univpm.it ,
[d] Department of Energy Conversion and Storage, Technical University of Denmark (DTU), Building 310, Fysikvej, DK-2800 Lyngby, Denmark, hlfr@dtu.dk

Abstract:

To mitigate climate change, a stronger reliance on renewable energy sources is foreseen, and Power-to-Hydrogen systems can be adopted to minimize curtailment losses derived from the intermittent nature of wind and solar power. Among different alternatives, alkaline water electrolysis is the most mature process for hydrogen production using sustainable electricity as its main energy source. The mathematical modelling of the alkaline electrolysis process is a crucial tool to improve green hydrogen production, energy conversion efficiency, sizing (model-based design) and thermal energy management. Although several studies have investigated alkaline electrolysis modelling, these analyses often neglect property variations along the stack area and its economic implications. In this work, the need for increasing the modelling complexity in system models by introducing a one-dimensional model of the alkaline electrolyzer cell/stack is investigated. With this, several operation parameter variations can be modelled, and among these, the internal temperature variation plays a crucial role in both technical and economic aspects. Results show that efficiency could vary between 58-70% while the Levelized cost of hydrogen is within the range of 1.3-1.6 €/kg, when various inlet-outlet temperature differences are considered. Furthermore, from both technical and economic aspects, the optimal temperature control of alkaline electrolysis is to maintain a very low-temperature difference (~1°C), from inlet to outlet, controllable with the alteration of the electrolyte flow rate.

Keywords:

Power-to-Hydrogen, Alkaline electrolysis, Temperature control, Levelized cost of hydrogen, Hydrogen production.

1. Introduction

The mitigation of the effects of climate change can be achieved through the integration of renewable energy sources into the electricity grid. However, the intermittent nature of these sources necessitates the use of storage and management mechanisms. One solution is the implementation of Power-to-X technologies, which involve the conversion of excess renewable electricity into other forms of energy that can be stored and utilized when needed. This facilitates the integration of intermittent renewable energy sources into the grid and supports the transition to a low-carbon energy system.

Water electrolysis can be divided into categories based on operating temperature: low-temperature electrolysis, working below 120°C, and high-temperature electrolysis. Among these technologies, alkaline water electrolysis, which utilizes a liquid electrolyte and Nickel-based catalysts, is the most mature and economically viable solution. However, it has lower efficiency and a limited current density range, as well as a constrained dynamic operating range [1].

Experimental investigation and modeling are essential tools for understanding the water electrolysis process. Based on the assumptions adopted, models can be classified as either data-driven or physical ones. Data-driven models rely on the mathematical treatment of experimental data and their parameters do not have a physical meaning, while pure physical models are based on the underlying physics of the electrolysis process

https://doi.org/10.52202/069564-0082

and all parameters have physical meanings. These models can be used to expand understanding of hydrogen production, energy conversion efficiency, sizing, thermal energy management and optimization.

The most known data-driven alkaline water electrolysis model is developed by Ulleberg [2], where the polarization curve, i.e., variation of voltage due to the current density through the alkaline cell, is modelled through six parameters. Several other researchers carried on this pathway, indeed Busquet et al. [3] carried on with the same approach using four parameters, while Ursua et al. [4] developed a sixteen parameters-based model. Since parameters are evaluated through experimental data, they can vary significantly even due to a slight variation of input data. Furthermore, more are parameters to be assessed, and more experimental variations are needed to generate unique data points. Indeed, with Ulleberg's model [2], the curve fitting requires following a seven-step procedure. Not to mention that these parameters do not have a physical meaning, thus is arduous to have a range estimation of these numbers.

As regards physical models, Hammoudi et al. [5] employed a multi-physical approach using Matlab Simulink® to carry out the physical model, considering both geometry and operating condition influence. They subsequently expanded this approach by coupling MATLAB-Simulink-SimPowerSystems®, validated using a Hydrogen Research Institute electrolyzer [6]. Such models can consider many aspects of the electrolysis process, however, but a high number of unknown physical parameters are needed, which are not easily achievable.

Both approaches have their opportunities and limitations, indeed, are applied to different cases of applications. Where at the system level. Fast and repeatable iterations, for a different set of operating conditions, are required, hence the data-driven models, once characterized are the most suitable ones; conversely, as for stack-level design, physical models are most suitable.

The temperature highly influences the operating conditions of the alkaline electrolyzers. To maintain it within the opportune range, several techniques can be used to control it. One approach is to use the water flow rate within the liquid electrolyte to maintain the desired temperature, such that the heat generated by the cell is efficiently dissipated or absorbed. When considering the techno-economic performance of an alkaline electrolysis system, it is crucial to carefully analyze the impact of temperature on the overall efficiency and cost of the system. For instance, Jang et al. [7] have built a model assessing electrolyte flow rate, needed as a temperature control measure, using a polynomial correlation, proposed by the same authors, based on temperature and current density, analyzing effects at various temperature differences, between inlet and outlet, of 1-3-5-10°C.

This work aims to cover the research knowledge gap by understanding the temperature dependencies of the alkaline electrolyzer system, solving the temperature evolution along the cells, and hence within the electrolyzer, based on a validated zero-dimensional/lumped model, extended to a one-dimensional model solving for mass and energy conservation, obtaining the electrolyte flow rate information by the physical meaning of the water electrolysis process, allowing to unlock the assessment of system performance at any temperature difference.

The main contributions of this work are the following:

- Propose and validate, with literature data, a semi-empirical alkaline water electrolysis model with four parameters, which can be applied to different types of electrolyzers.
- Formulation of a one-dimensional water electrolysis model, based on the physical process, solving ordinary differential equations. Which can assess the evolution of all operating parameters, such as temperature and pressure, illustrating its comparison with other dimensions models.
- Techno-economic assessment of the temperature control, by the sense of heating mass (electrolyte flow rate) variation, at a continuous range of gap temperatures.

The paper is structured as follows: Section 2 describes the methodology adopted in this work, highlighting the proposed semi-empirical model, validated and extended to a one-dimensional model, while Section 3 describes the results obtained and finally the conclusion of the work is reported in Section 4.

2. Methods

In this section, firstly a novel data-driven model, for Potassium Hydroxide (KOH) electrolyte-based alkaline electrolysis modelling, is proposed. Secondly, the model has been fitted with empirical data provided by literature, where four distinct datasets have been tested; Furthermore, the extension into the one-dimensional model, solving ordinary differential equations of mass, and energy balancing, has been discussed, concluding finally the indicators adopted for the technical and economic comparison of the work.

2.1. Alkaline electrolyzer modelling

Despite different assumptions and refinements present in alkaline electrolyzer modelling, they share the same goal, which is to describe accurately the polarization curve, indeed it is the curve which underlines the voltage (V_{cell}) variation due to the fluctuations of the current density (j), and it can be described with the following equation:

https://doi.org/10.52202/069564-0082

$$V_{cell} = V_{rev} + \eta_{act} + \eta_{ohm} + \eta_{bubble} \quad (1)$$

Where the V_{cell} is the voltage of a single electrolysis cell, V_{rev} is the reversible voltage i.e. the minimum electrical potential to have the electrolysis process going, η_{ohm} the ohmic overvoltage comprising both electrolyte and electrodes overpotential, η_{act} the activation overpotential of both electrodes and finally η_{bubble} is the overpotential, caused by bubble formation from liquid electrolyte.

Each term of the equation (1). can be modelled in different ways, based on the approach and researchers' decisions. It was found that almost all commercial alkaline electrolyzers adopt bipolar electrical configuration, meaning the cells are electrically connected in series since it allows to have higher utilization of the cell area, as reported in [8], therefore the whole electrolyzer has the same current of the cell level, while the overall voltage of the stack is the sum of all the cell's voltages. Furthermore, the polarization curve provides insights into hydrogen production as well as conversion efficiency.

The proposed model describes the polarization curve as follows:

$$V = V_{rev} + \left(\frac{1}{\alpha}\right)\frac{RT}{2F} ln\left(\frac{j}{j_0}\right) + j \cdot \left(\frac{\delta_{el}}{\sigma_{el}}\right) \quad (2)$$

$$j_0 = B \cdot \exp\left(-\frac{E_a}{RT}\right); \ln(j_0) = \ln(B) + \left(-\frac{E_a}{R}\right) \cdot \frac{1}{T} \quad (3)$$

Where V_{rev} can be assessed using the Nernst equation, which changes based on electrolyzer operating conditions, as reported in [9]. While for σ_{el}, using KOH electrolyte, is assessed through the empirical equation investigated by experiments performed by Gilliam et al.[10], and finally j_0, exchange current densities for both electrodes can be described through the Arrhenius equation.

Thus, four parameters remain to be estimated through the alkaline electrolyzer operating data. They are respectively: α, $\ln(B)$, $\left(\frac{E_a}{R}\right)$ and δ_{el}. Furthermore, several simplifications have been made to obtain a simple and versatile for different types of electrolyzers. Indeed, (i) both electrodes' activation overpotentials are grouped with a single Tafel equation, (ii) both diaphragm and electrolyte ohmic overpotential are grouped, due to the lack of information on the diaphragm material composition and experimental correlation, and finally (iii) the bubble formation overpotential, since its effects on activation overpotential are reduced the activation area and changes in electrolyte ionic conductivity, both effects are implicitly taken into account thanks to the parameter-estimation, through the electrolyzer operating data.

2.1.1. Model validation

The proposed model is further tested and validated, using the experiments presented in the literature by different researchers, to represent different types of alkaline electrolyzers with different set-ups of operating conditions. Such operating conditions are namely i) temperature, ii) KOH concentration, and iii) pressure. Additionally, the model's robustness, i.e. its ability to have reasonable accuracy, dealing with the minimum quantity of the data available, has been also tested.

The procedure of calibration of the model, based on the type of the electrolyzer with its results, is illustrated in Figure 1, which can be divided into 3 phases:

- Experimental data processing, ensuring at least 6 data points are present, ensuring a good accuracy of the model. If more data is available, they can be also included, however, not all available data should be used, to prevent the over-fitting problem.
- The pre-processed data is then inserted into a curve-fitting framework, commonly used ones are Matlab and Python adopting the proposed model, assessing 4 calibrating parameters ($\delta_{el}, \alpha, \ln(B), -E_a/R$),
- As a consequence of the previous step, the model is now defined, and as such, polarization curves at temperatures, different from the ones used to calibrate the parameters can be obtained and used as validation data.

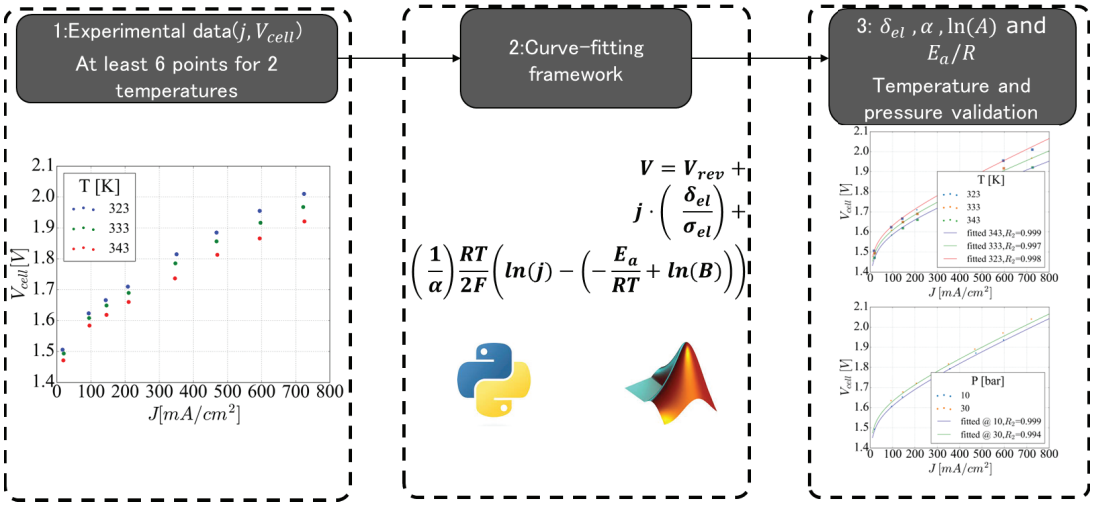

Figure 1. Parameters estimation procedure. Divided into three phases: 1) collection of experimental data at different temperatures, 2) parameter estimation and 3) temperature and pressure influence validation.

2.1.2. Extension of lumped model: one-dimensional model

The proposed model, describing the water electrolysis at the single cell level, can be called a zero-dimensional model/lumped model, in the sense that it assesses the performance of the cell with only a single set of operating conditions, meaning no variation of i) temperature ii) pressure and iii) KOH concentration along e.g. the flow direction and the temperature is considered.

It is possible to extend the lumped model to a half-dimensional model, where two sets of operating conditions are considered, namely inlet and outlet ones. However, this approach has an evident drawback, which is the need for information in advance about the outlet conditions, which is not always available, but can be assumed through e.g. a linear variation of parameters along the stack e.g. current density.

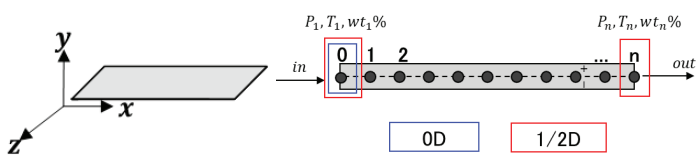

Figure 2. Alkaline electrolysis cell models. With the x-axis as the flow direction.

Therefore, in this study, such a model is further extended into a one-dimensional model, obtaining a complete cell performance evaluation (Figure 2), as an extension of zero-dimensional and half-dimensional ones, which can be applied also to stack-level once defined the electrolyzers cells interconnection, that for this study, bipolar configuration, i.e. cells electrically connected in series, is adopted, as illustrated by Figure 3.

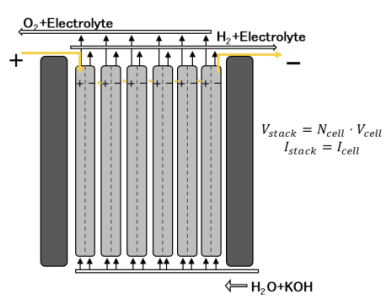

Figure 3. Alkaline electrolyzer bipolar configuration 1D model.

As a modeling assumption, it is considered that all properties vary only along the flow direction, which is the x axis, ignoring their contribution in other axes, in other meaning:

https://doi.org/10.52202/069564-0082

$$\frac{d\Gamma}{dy} = 0; \frac{d\Gamma}{dz} = 0 \tag{4}$$

Where Γ represents a generic physical property. The one-dimensional model proposed uses discrete element modeling, solving differential equations, wherein each element (i), molar flow rate ($\dot{n}_{H2}$), and temperature (T) are solved:

$$\frac{d\dot{n}_{H2}}{dx} = \frac{J_i}{2F} \cdot \Delta \tag{5}$$

$$\frac{dT}{dx} = \frac{(V - V_{th}) \cdot J_i}{\dot{n}_e \cdot Cp_e + \dot{n}_{H2} \cdot Cp_{H2} + \dot{n}_{O2} \cdot Cp_{O2}} \cdot \Delta \tag{6}$$

$$i = 0,1,2,3 \ldots n; \Delta = \text{const} \tag{7}$$

While different parameters are defined in the nomenclature at the end of the paper, such equations represent the molar mass, and energy balance along the x-axis, where Δ represents the cell width (cell dimension in z-axis), which is constant. While for the standard chemical species, their thermodynamical properties, like specific heat (Cp) can be consulted or calculated using the well-known empirical equations from the database of NASA [11]. The electrolyte, composed of water and a certain mass fraction of KOH, its thermal properties can be assessed using empirical formulas reported in the [12], obtained as results of experiments, where for this study, Zaytsev empirical relationship has been used [13]:

$$Cp_{el} = k_1 + k_2 \ln\left(\frac{T_{\circ C}}{100}\right) + (k_3 + k_4 \cdot wt + 8 \cdot T_{\circ C}) \cdot wt \tag{8}$$

With the obtained Cp_e is expressed in [J/kg K], to converted into [J/mol K] using the following equation:

$$Cp_{e,mol} = Cp_e \cdot M_e \tag{9}$$

$$\sum \frac{wt_i}{M_i} = \frac{1}{M_{tot}} \sum \frac{n_i}{n_{tot}} \cdot \frac{M_i}{M_i}; M_{tot} = \frac{1}{\sum \frac{wt_i}{M_i}}; \; M_e = \frac{1}{\frac{wt}{M_{KOH}} + \frac{(1-wt)}{M_{H2O}}} \tag{10}$$

$$wt = \frac{m_{KOH}}{m_{KOH} + m_{H2O}} \tag{11}$$

The flowchart of the proposed 0D model, extension to the 1D cell model, and finally into the 1D stack model, is illustrated in Figure 4.

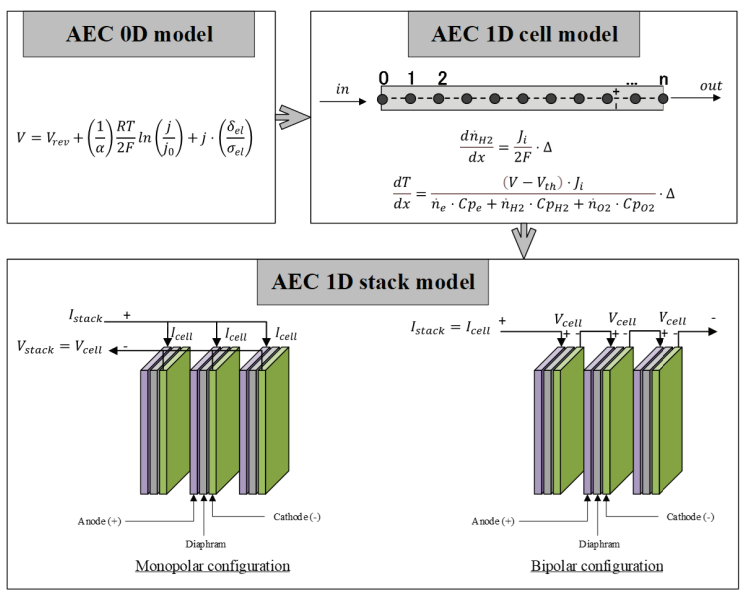

Figure 4. Alkaline 1D stack model flowchart. Starting with the single cell 0D model, extended to 1D cell model, solving mass and thermal balance, and finally 1D stack model, based on the electrical configuration among cells.

2.2. Technical and economic comparison

To have an overview of different models' comparison, in terms of both technical and economic perspectives, the assumption of having inlet and outlet temperature is the same for all models, whereas the 0D model considers only the inlet temperature.

$$0D: T_{inlet}; J = J_{inlet} = f(T_{inlet}, V, wt, p) \quad (12)$$

$$1/2D: T_{\text{inlet}}, T_{outlet}; J = J_{avg} = \frac{J_{inlet} + J_{outlet}}{2} \quad (13)$$

$$1D: T_i; i = 0, \dots n; J = J_{avg} = \frac{\int J_{i \cdot dx}}{n \cdot \Delta X} \quad (14)$$

$$Area = x \cdot width; x = 0, 1 \cdot \Delta x \dots, n \cdot \Delta x \quad (15)$$

Furthermore, for the technical comparison among different models, since the temperature-controlling components are included in this analysis, namely heat exchangers and pumps, the interconnection of these parts with the electrolyzer is described in Figure 5. Where heat exchangers, have the objective to cool the outlet electrolyte, warmed up by the inefficiencies, down to the inlet setting temperature. While temperature control can be done by controlling the flow rate of the inlet water, as described in equation (6) and equation (8) the increase of the water flow rate can lower the temperature gap, hence increasing the cell's overall working efficiency, however, with an expense of a higher required power for the electrolyte circulation. The pressure gap is assumed to be equal to 1 bar for the sake of simplicity.

The system integration between alkaline electrolyzer and other components of the plant is illustrated through the flow diagram reported in Figure 5, despite having multiple components present in the plant, not all of them have been modelled in the present study, as they are out of the scope of the objective.

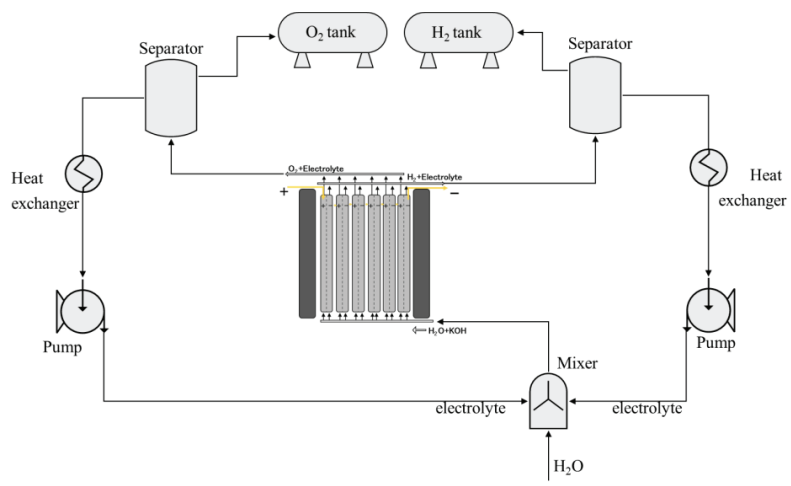

Figure 5. Systems connections. Illustrating auxiliary systems to be coupled with electrolyzer stack.

Indeed, the components that accounted for the evaluation of the temperature control, besides the electrolyzer stack itself, are water pumps and heat exchangers, where their characteristics, used for this work, are reported in Table 1.

Table 1. Model parameters.

Pheobus electrolyzer		Reference
Cell area (m2)	0.25	[2]
#n cells	21	[2]
Operating pressure (bar)	7	[2]
Nominal power (kW)	26	[2]
Unitary cost (€/kW)	830	[14]
Stack lifetime (years)	10	[14]
Water pump		
Efficiency	0.7	[14]
Input power	$P = \eta_{pump} \cdot \Delta P \cdot Q_e$	[-]

https://doi.org/10.52202/069564-0082

Pressure Gap	1 bar	[-]
Cost	60 €/(kg/s)	[14]
Heat exchanger		
Cost (€)	$C = C_1 \left(\frac{A_{HEX}}{0.093}\right)^{0.78}$	[14]
C_1	110 €/m^2	[14]
U (W/m2 K)	700	[14]
ΔT_{HEX} (K)	5	[-]
A_{HEX} (m2)	$A_{HEX} = \frac{\dot{n}_{H2O} \cdot M_{H2O} \cdot Cp_{H2O} \cdot \Delta T_{H2O}}{U \cdot \Delta T_{HEX}}$	[-]
Lifetime (years)	15	[14]
Levelized Cost of Electricity		
€/MWh	20-60	[14]

As evaluation indicators, exploiting the temperature effects, system-level efficiency, and levelized cost of the produced hydrogen are adopted to assess the temperature influence. And these indicators assessment criteria are reported in the following equations:

$$\eta_{tot} = \frac{N_{cell} \cdot \dot{n}_{H2_{cell}} \cdot LHV_{H2}}{P_{el} + P_{pump}} \tag{16}$$

$$LCOH = \frac{CAPEX_{el,a} + CAPEX_{HEX,a} + CAPEX_{WP,a} \cdot + LCOE \cdot E_{elc}}{m_{H2}} \tag{17}$$

Where all investment costs ($CAPEX$), that depend on the nominal size of the technology, are actualized while E_{el} is the electrical energy consumed to produce the m_{H2}.

3. Results & discussions

Different types of results are reported in this section, firstly the results regarding the validation of the novel are illustrated, to be followed with the comparison of different dimensionality of the model, and finally the technical andeconomic analysis of the temperature control effects, are discussed.

3.1. Ability for the model to fit data

The proposed model proved its validity and robustness; indeed, the results show that only six data points, three data points for each, and two temperatures are needed, to capture the temperature and the current density dependency. Of course, the parameters are strictly dependent on the data points used to estimate them, however, the difference is not significant, and they are listed in Table 2.

Table 2. Parameters for the datasets analyzed.

	Experiments conditions		**Calibrated parameters**				
	p	T	wt	δ_{el}	α	$-E_a/R$	$\ln(\mathrm{B})$
Units	$[bar]$	$[°C]$	$[-]$	$[cm]$	$[-]$	$[K]$	$\left[\ln\left(\frac{mA}{cm^2}\right)\right]$
Sakas [15]	16	59.6-61.15-70	0.25	0.3914	0.1253	-6330	13.11
Ulleberg [2]	7	30-40-50-60-70-80	0.30	0.6637	0.1726	-5331	9.184
Sanchez [16]	7	55-65-75	0.35	0.5711	0.1181	-3592	4.768
Groot [17]	30	50-60-70	0.28	0.2716	0.2764	-3906	3.864

During the parameter estimation process, the dataset is split into two separate datasets. Namely train and test datasets, to prove the model's robustness. Indeed, the training dataset, i.e. the data used to find parameters, is randomly selected, with the only constraint that they need to be at least six data points, from at least two different operating temperatures. The results of the estimation, illustrating the model's wide applicability, are reported in Figure 6.

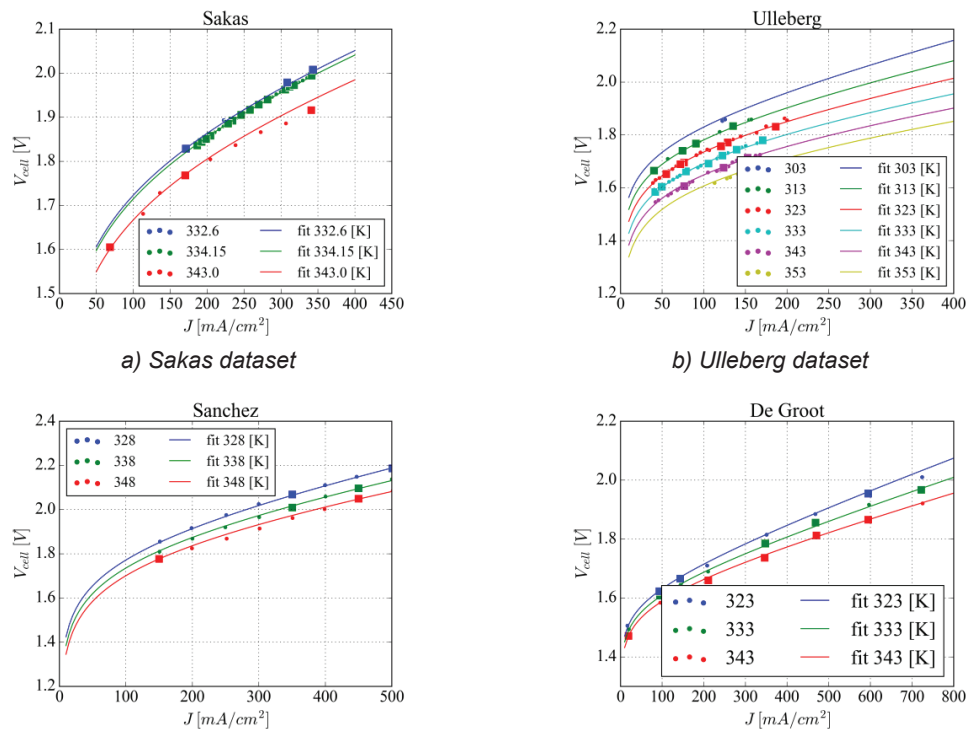

a) Sakas dataset *b) Ulleberg dataset*

c) Sanchez dataset d)De *Groot* dataset

Figure 6. Parameter estimation and validation with temperature variation. Where squared-dotted data are from the training dataset while the circle ones are from the test dataset.

Whereas the temperature dependence is explicitly highlighted, in activation overpotential, other operating conditions influence, namely KOH weight concentration and pressure are implicitly considered, through the ohmic overpotential and reversible voltage, respectively.

3.1. Accuracy of model dimensionality

The one-dimensional model is controlled by voltage; hence the voltage is an input parameter of the model. Whereas the current density, thus also the hydrogen production is an output data from the model.

The benefit of having a one-dimensional model resides in the possibility to perform analysis at different temperatures, between the inlet and outlet of the cell. Indeed, Figure 7 is reported the results of the 1D model for a 0.30x0.30 m cell, working at 1.8V, with an outlet temperature fixed at 80 °C with different gap temperatures, namely 1-2-10 °C.

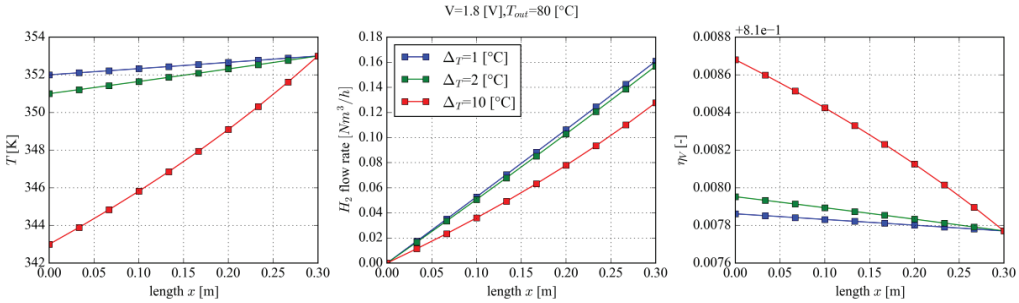

Figure 7. 1D model at 1-2-10 °C temperature difference. Illustrating namely i) temperature, ii) hydrogen production and iii) voltage efficiency along the cell. Where the outlet temperature is kept constant. Despite having a higher temperature difference achieves a higher efficiency, the produced hydrogen flow is lower.

https://doi.org/10.52202/069564-0082

A comparison of the different dimensionality of the model is illustrated in Figure 8. The 1D model is used as a reference, as this is considered the most accurate. The current density at a fixed potential of 1.8 V is compared. This is done at different flow rates of the electrolyte through the stack for cooling, resulting in different temperature increases over the stack.
The comparison shows that the 0D model is always underestimating the current density and thus the hydrogen production rate. The 1/2D model, in contrast, is overestimating the two. Furthermore, with an operating temperature of 80°C (353 K) and voltage of 1.8 V, considering the one-dimensional model as the benchmark, with a gap temperature of 5°C between the inlet and outlet, while the half-dimensional model's deviation is almost neglectable (0.75%), the zero-dimensional model has a significant deviation, underrating about 11% the hydrogen production.

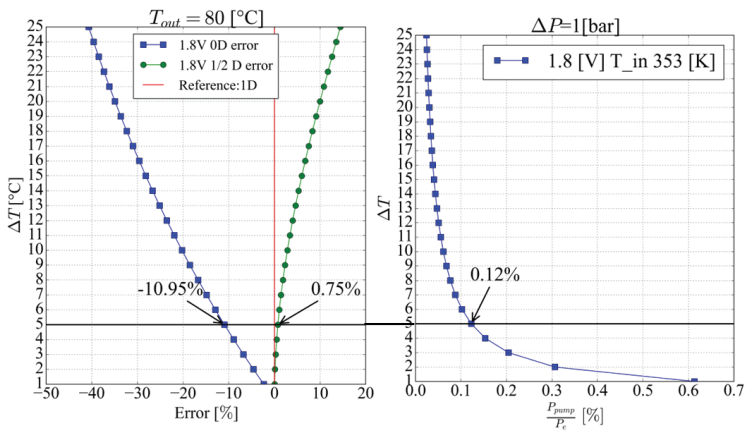

Figure 8. Models' comparison at different temperature increase over the stack. Where error is the difference between the models' average current density, compared with the 1D model's average current density, in percentage.

Regarding temperature effects, with a temperature increase, between the inlet and outlet of the electrolyzer stack, larger than 1°C, the overall efficiency (defined in equation (16)) remains almost constant at a value of 0.69 (Figure 9); and since the model is fixing voltage as input, results are implying that, after such threshold, the influence of the water pump energy consumption, which depends on the water flow rate, required to control the operating temperature, is almost neglectable, compared to the energy absorbed by the electrolyzer.

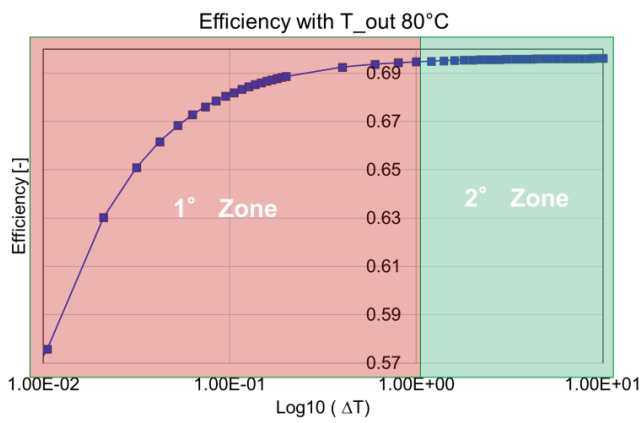

Figure 9. Influence of temperature difference (inlet to outlet) in system efficiency. Where the outlet temperature is set as 80°C.

As for the economic aspect, as illustrated in Figure 10, there's a clear zone (2° zone), where the LCOH stays at its minimum level, indeed, such range is around the gap temperature of 1°C, independently from the LCOE adopted, however, with a slope of LCOH (defined in equation (17)) decrease/increase different in two cases. However, the LCOH are higher in the other two zones (1° zone and 3° zone), due to different reasons, while for the 1° zone, the cause is the high operational cost due to the water pump energy absorption, for the 3°

zone instead, is due to a drop in current density, indeed with a higher gap temperature, the overall hydrogen production, results to be lower and lower.

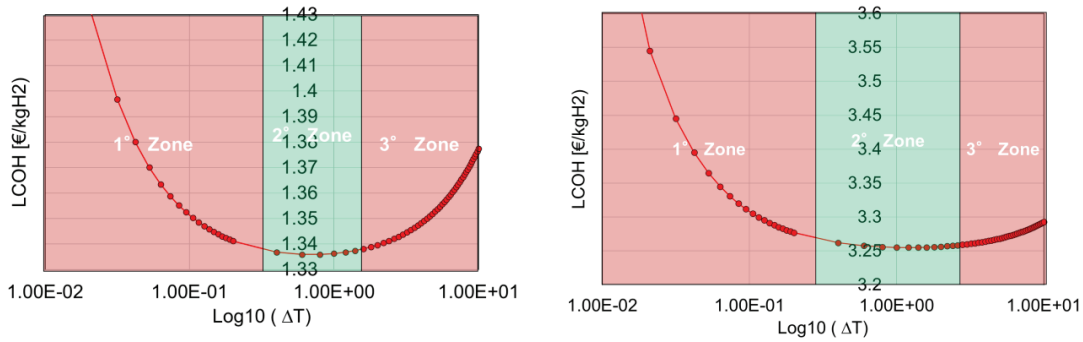

a) LCOH with minimum LCOE *b) LCOH with maximum LCOE*

Figure 10. Influence of temperature difference (inlet to outlet) in the levelized cost of hydrogen. Where the outlet temperature is set as 80°C

There are several limitations of the proposed model. It does not consider the faraday efficiency, because of the lack of an aligned approach to it in literature, furthermore, the water vapor formation has not been properly addressed. Nevertheless, since the objective of the work is to assess the temperature influence and its control, such limitations would not change the discussed results, yet they can certainly be subject to further investigation.

4. Conclusion

In this study, the assessment of the alkaline operating temperature effects and its control, from both technical and economic aspects, has been carried out.

To seize these quantities of the electrolysis process, a novel alkaline cell model is proposed. The model was fitted to various data from the literature and shown to provide good fits for all the considered measurements. The model included only four parameters, which are a combination of the physical parameters as well as empirical parameters describing certain physical phenomena.

Furthermore, after validating the proposed cell model, it has been extended to one-dimensional modelling, based on the finite element approach, including the mass and energy balance, which provides the evolution of different operating parameters along the cell, such as temperature. To understand the impact of model accuracy on system models, a comparison of different model refinements was conducted, i.e. a 0D, 1/2D and a 1D model. The 0D model is significantly underestimating the hydrogen production (-11%), while the 1/2D model has a slight overestimation (+0.75%), as compared to the more accurate 1D model.

Furthermore, the effect of electrolyte rate on the overall efficiency was investigated - both technically and economically. There are clear benefits of increasing the flow rate of the electrolyte to keep temperature increase over the stack close to 1°C.

The efficiency with increasing flow rates will go down, however, remains constant if the temperature increase is kept above 1°C. Economically there is an optimum flow rate, where losses from the pumping of electrolytes and losses in the stack due to higher resistance at lower temperatures are balanced.

Although the global trend of the LCOH does not change, with different values of LCOE (20-60 €/MWh), its value is quite different, where for 20 €/MWh, it can be 1.33-1.43 €/kg_{H2}, alternately, 3.25-3.6 €/kg_{H2} for 60 €/MWh.

Nomenclature

$\dot{n}$	Molar flow rate, mol/s
LHV	Low heating value, J/mol
A	Area, m^2
B	Arrenhius constant, mA/cm^2
$CAPEX$	Capital Expenditure, €
E	Energy, kWh
F	Faraday constant, 96500 C/mol
H	Enthalpy, J/mol

https://doi.org/10.52202/069564-0082

I	Current, A
$LCOE$	Levelized Cost of Energy, €/kWh
$LCOH$	Levelized Cost of Hydrogen, €/kg
M	Molarity of the solution, mol/l
N	Number,-
P	Power, W
R	Universal gas constant, 8.314462618 J/mol K
T	Temperature, K
U	Heat transfer coefficient, W/m^2 K
V	Voltage, V
a	Water activity, -
j	Current density, A/m^2
m	mass, kg
n	Number of elements,-
p	Pressure, bar
v	Velocity, m/s
wt	Weight concentration, [0.0 - 1.0]

Greek symbols

α	Charge transfer coefficient, -
δ	Reaction distance, cm
η	Overpotential, V
σ	Ionic conductivity, S/cm
Δ	Cell width, m
Γ	Generic property, -

Subscripts and superscripts

$\%$	Percentage
H_2O	Water
$°C$	Celsius
$H2$	Hydrogen
HEX	Heat exchanger
KOH	Potassium Hydroxide
$O2$	Oxygen
X, a	Actualized cost of X technology
act	Activation
$bubble$	Bubbles
$cell$	Single cell
d	Diaphragm
el	Electrolyte/Electrolyzer
elc	Electricity
$inlet$	Cell inlet
ohm	Ohmic
$outlet$	Cell outlet
$pump$	Water pump
rev	Reversible
th	Thermo-neutral
v	Vapor

References

[1] Grigoriev SA, Fateev VN, Bessarabov DG, Millet P. Current status, research trends, and challenges in water electrolysis science and technology. Int J Hydrogen Energy 2020;45:26036–58. https://doi.org/10.1016/j.ijhydene.2020.03.109.

[2] Ulleberg Ø. Modeling of advanced alkaline electrolyzers: a system simulation approach. Int J Hydrogen Energy 2003;28:21–33. https://doi.org/10.1016/S0360-3199(02)00033-2.

[3] Busquet S, Hubert CE, Labbé J, Mayer D, Metkemeijer R. A new approach to empirical electrical modelling of a fuel cell, an electrolyser or a regenerative fuel cell. J Power Sources 2004;134:41–8. https://doi.org/10.1016/j.jpowsour.2004.02.018.

[4] Ursúa A, Sanchis P. Static-dynamic modelling of the electrical behaviour of a commercial advanced alkaline water electrolyser. Int J Hydrogen Energy 2012;37:18598–614. https://doi.org/10.1016/j.ijhydene.2012.09.125..

[5] Hammoudi M, Henao C, Agbossou K, Dubé Y, Doumbia ML. New multi-physics approach for modelling and design of alkaline electrolyzers. Int J Hydrogen Energy 2012;37:13895–913. https://doi.org/10.1016/j.ijhydene.2012.07.015.

[6] Henao C, Agbossou K, Hammoudi M, Dubé Y, Cardenas A. Simulation tool based on a physics model and an electrical analogy for an alkaline electrolyser. J Power Sources 2014;250:58–67. https://doi.org/10.1016/j.jpowsour.2013.10.086.

[7] Jang D, Choi W, Cho HS, Cho WC, Kim CH, Kang S. Numerical modeling and analysis of the temperature effect on the performance of an alkaline water electrolysis system. J Power Sources 2021;506. https://doi.org/10.1016/j.jpowsour.2021.230106.

[8] Ursúa A, Gandía LM, Sanchis P. Hydrogen production from water electrolysis: Current status and future trends. Proceedings of the IEEE, vol. 100, Institute of Electrical and Electronics Engineers Inc.; 2012, p. 410–26. https://doi.org/10.1109/JPROC.2011.2156750.

[9] Olivier P, Bourasseau C, Bouamama PB. Low-temperature electrolysis system modelling: A review. Renewable and Sustainable Energy Reviews 2017;78:280–300. https://doi.org/10.1016/J.RSER.2017.03.099.

[10] Gilliam RJ, Graydon JW, Kirk DW, Thorpe SJ. A review of specific conductivities of potassium hydroxide solutions for various concentrations and temperatures. Int J Hydrogen Energy 2007;32:359–64. https://doi.org/10.1016/J.IJHYDENE.2006.10.062.

[11] Mcbride BJ, Zehe MJ, Gordon S. NASA Glenn Coefficients for Calculating Thermodynamic Properties of Individual Species. 2002.

[12] le Bideau D, Mandin P, Benbouzid M, Kim M, Sellier M. Review of necessary thermophysical properties and their sensivities with temperature and electrolyte mass fractions for alkaline water electrolysis multiphysics modelling. Int J Hydrogen Energy 2019;44:4553–69. https://doi.org/10.1016/J.IJHYDENE.2018.12.222

[13] Zaĭtsev ID, Aseev GG. Properties of Aqueous Solutions of Electrolytes. Undefined 1992;30:30-4415-30–4415. https://doi.org/10.5860/CHOICE.30-4415.

[14] Nami H, Rizvandi OB, Chatzichristodoulou C, Hendriksen PV, Frandsen HL. Techno-economic analysis of current and emerging electrolysis technologies for green hydrogen production. Energy Convers Manag 2022;269:116162. https://doi.org/10.1016/J.ENCONMAN.2022.116162.

[15] Sakas G, Ibáñez-Rioja A, Ruuskanen V, Kosonen A, Ahola J, Bergmann O. Dynamic energy and mass balance model for an industrial alkaline water electrolyzer plant process. Int J Hydrogen Energy 2022;47:4328–45. https://doi.org/10.1016/J.IJHYDENE.2021.11.126.

[16] Sánchez M, Amores E, Rodríguez L, Clemente-Jul C. Semi-empirical model and experimental validation for the performance evaluation of a 15 kW alkaline water electrolyzer. Int J Hydrogen Energy 2018;43:20332–45. https://doi.org/10.1016/j.ijhydene.2018.09.029

[17] de Groot MT, Kraakman J, Garcia Barros RL. Optimal operating parameters for advanced alkaline water electrolysis. Int J Hydrogen Energy 2022. https://doi.org/10.1016/j.ijhydene.2022.08.075